Eur. Phys. J. A **20**, 39–44 (2004)
DOI 10.1140/epja/i2002-10318-y

THE EUROPEAN PHYSICAL JOURNAL A

# The origin of doublet bands observed in A $\sim$ 130 nuclei

C.M. Petrache[a]

Department of Physics, University of Camerino, and INFN, Sezione di Perugia, Italy

Received: 10 October 2002 /
Published online: 17 February 2004 – 

**Abstract.** The results obtained with the GASP array in the $A \sim 130$ mass region are reviewed, emphasizing the study of excited highly deformed bands and their decay out, the discovery of chiral doublet bands in the odd-odd Pr nuclei and of stable triaxial bands in Nd nuclei close to the $N = 82$ shell closure. The very recent studies of nuclei near the proton drip line are described. A discussion of the origin of the various doublet bands observed in odd-odd nuclei of the $A \sim 130$ mass region is presented.

**PACS.** 23.20.Lv Gamma transitions and level energies – 21.10.-k Properties of nuclei; nuclear energy levels – 21.60.Ev Collective models – 25.70.-z Low and intermediate energy heavy-ion reactions

## 1 Introduction

The spectroscopic study of neutron-deficient nuclei in the $A \sim 130$ mass region undertaken at the Legnaro National Laboratory with the GASP array led to numerous achievements on various fields of interest in both the high- and low-spin regime: the study of highly deformed bands which helped to understand the main excitations at high deformation [1–13], the discovery of the decay-out of these bands in a series of six Nd nuclei which allowed the extraction of the neutron pairing gap $\Delta_\nu$ in the second well [12,13], the discovery of doublet bands in odd-odd nuclei which were interpreted as the manifestation of chiral or pseudospin symmetry in nuclei [14–17], the evolution of triaxiality which led to the discovery of stable triaxial bands at the highest spins when approaching the $N = 82$ shell closure [18–20]. For all studied nuclei, we established very complete level schemes on the basis of data obtained in heavy-ion–induced reactions, being able to efficiently identify very weak transitions in the energy range from about 20 keV to several MeV. All these exciting results were obtained with the aid of very efficient ancillary detectors used in conjunction with the GASP array in selecting the various reaction channels, like the ISIS charged-particle detector, the CAMEL recoil mass spectrometer and the neutron ring.

## 2 The decay-out of highly deformed bands and stable triaxiality in Nd nuclei

The most extended studies of highly deformed bands have been performed for Nd nuclei, leading to the observation of linking transitions over a series of six nuclei. The discovery of the decay-out in the Nd sequence of nuclei lead to the determination of the excitation energy, spin and parity of the highly deformed states. From these studies we could conclude that the highly deformed bands have different decay-out patterns depending i) on the type of nucleus (even-even or odd-even) and ii) on the parity of the highly deformed band. The bands in the odd-even Nd nuclei decay out towards low-lying normal-deformed states via $E2$ transitions ($^{133}$Nd), $E2$ plus $E1$ transitions ($^{135}$Nd) and cascades of $E2$ plus $M1$ transitions ($^{137}$Nd) (see fig. 1). The highly deformed bands in even-even Nd nuclei, which are built on two quasi-particle neutron excitations, are based on two types of configurations, which lead to either negative parity (the yrast bands observed in $^{132,134,136}$Nd which are shown on fig. 2) or positive parity (the excited bands observed in $^{132,134}$Nd). The negative-parity bands decay in two steps via $E2$ + enhanced $E1$ transitions with strengths of $\sim 10^{-3}$ W.u., whereas the positive-parity bands decay in one step via $E2$ transitions with strengths of $\sim$ 1 W.u. The conclusion was drawn that the mixing with the normal-deformed states plays a more important role than the sliding between different deformations via the pairing interaction. The interaction matrix elements and mixing amplitudes between normal- and highly deformed bands in Nd nuclei were deduced in the decay-out region and at high spins, showing that the barrier at the point of decay out disappears.

The discovery of discrete linking transitions in the series of six Nd nuclei from $^{132}$Nd to $^{137}$Nd, allowed to estimate the pairing strength in the highly deformed configuration, from the odd-even mass differences. Using a first-order Taylor expansion [21] and the three-point formula [12], we extracted the experimental neutron pairing

[a] e-mail: costel.petrache@unicam.it

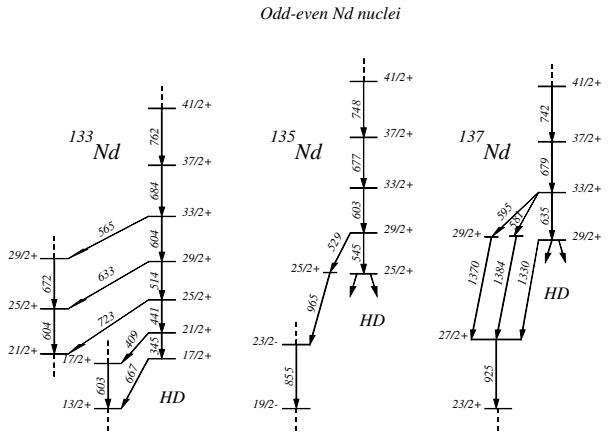


**Fig. 1.** Decay-out of the highly deformed bands in odd-even Nd nuclei.

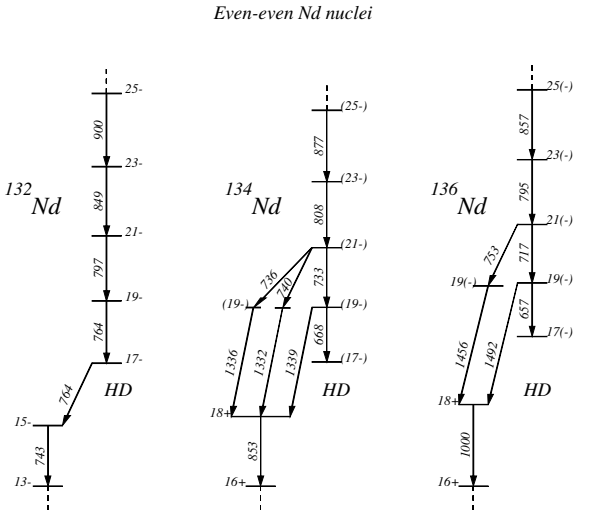


**Fig. 2.** Decay-out of the negative-parity highly deformed bands in even-even Nd nuclei.

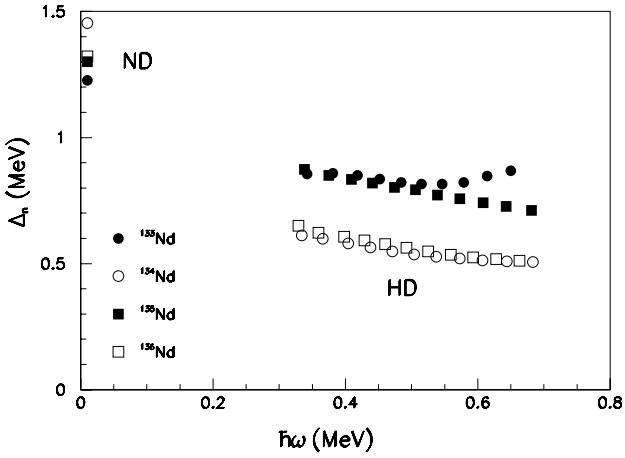


**Fig. 3.** Experimental neutron pairing gaps for the normal-deformed ground states and for the highly deformed configurations in Nd nuclei.

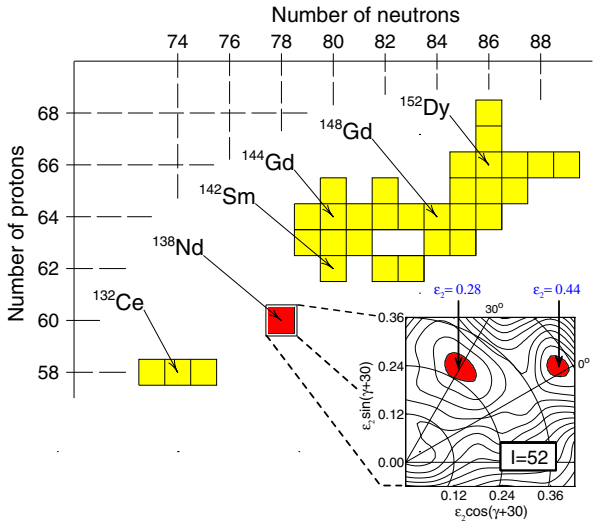


**Fig. 4.** Extract of the nuclear $(N, Z)$-chart indicating those nuclei where superdeformed bands have been observed. Note how the nucleus $^{138}$Nd would "fill the gap" between the Ce and the Sm/Eu regions of superdeformation. The calculated potential energy surface for this nucleus (with a contour line separation of 0.5 MeV) shows one minimum at $\varepsilon_2 = 0.28$ ($\gamma \approx 30°$), corresponding to presently observed highly deformed bands in Nd nuclei, and then the superdeformed minimum at $\varepsilon_2 = 0.44$.

gap in the normal-deformed ground state and in the highly deformed configurations for two odd-even and two even-even Nd nuclei (see fig. 3). The pairing gap values for the highly deformed configurations, are reduced by approximately a factor of 2 with respect to the values for the normal-deformed ground states ($\Delta_n \sim 0.6$–$0.7$ MeV) and remain rather constant in a wide range of frequencies. In the normal-deformed case, the pairing gaps of the odd-even nuclei are smaller than those of the even-even ones, whereas in the highly deformed configurations the opposite is true: the pairing gaps of the two-quasiparticle configurations present in even-even nuclei is smaller than the pairing gaps of the one-quasiparticle configurations present in odd-even nuclei. This peculiar feature is due to the blocking effects, which are stronger in the two-quasiparticle configurations based on intruder orbitals of different nature ($\nu i_{13/2}$ and $\nu f_{7/2}$) than in the one-quasiparticle $\nu i_{13/2}$ configurations.

One of the last achievements we obtained in the study of the Nd nuclei is the discovery of bands with stable triaxiality up to the highest states in $^{138,139}$Nd [20]. The observed bands have considerably smaller collectivity than the triaxial bands identified in the other $A \sim 130$ nuclei, and are based on oblate-triaxial shape with $\gamma \sim +30°$ rather than the prolate-triaxial shape with $\gamma \sim -30°$ present in the lighter nuclei (see fig. 4).

## 3 Study of odd-odd Pr nuclei

In the odd-odd nuclei of the $A \sim 130$ mass region the prevalent structures are semi-decoupled deformed rotational bands built on $\pi h_{11/2} \otimes \nu h_{11/2}$, $\pi g_{7/2}/d_{5/2} \otimes \nu h_{11/2}$ and $\pi h_{11/2} \otimes \nu g_{7/2}$ configurations [14–17,22]. However,

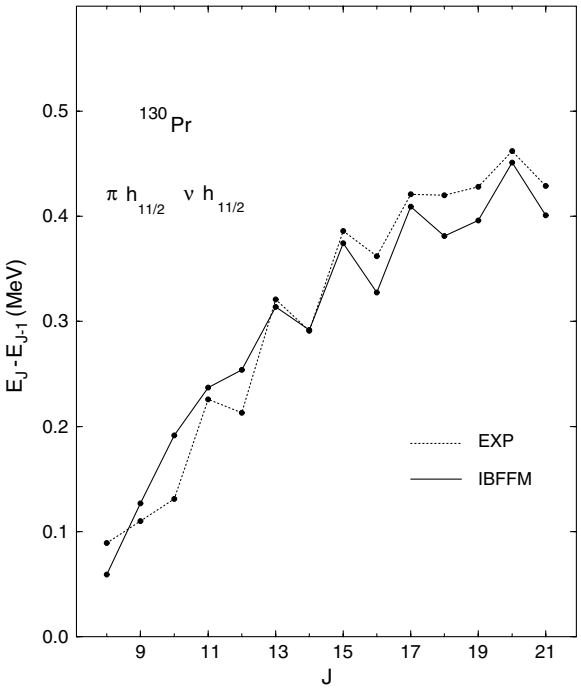


**Fig. 5.** $E_J - E_{J-1}$ *vs.* $J$ plot for band 2 in $^{130}$Pr.

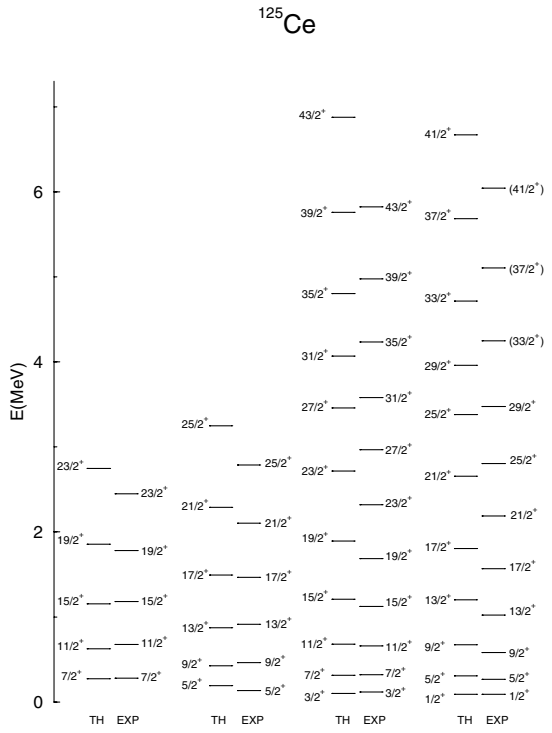


**Fig. 6.** The positive-parity states of bands 2 and 3 in $^{125}$Ce compared with the results of the IBFBPM calculation.

there are several cases in which also weakly populated double-decoupled bands were observed, with assigned configurations involving the $\pi g_{9/2}$ and $\nu f_{7/2}/h_{9/2}$, $\nu i_{13/2}$ configurations [10,11,14,15,17]. From the study of the odd-odd Pr nuclei we obtained important information on the signature inversion phenomenon (see fig. 5 taken from ref. [16]) through the interpretation in the framework of the Interacting Boson-Fermion-Fermoin model [15,16,22], on the competition between prolate and oblate shapes in the $\gamma$-soft nuclei by means of Total Routhian Surface calculations [11,14,15], and, more recently, on the possible existence of chiral doublet bands predicted by 3D Tilted Axis Cranking calculations [17]. A discussion of the observed doublet bands in $^{134}$Pr and $^{128}$Pr will be given in sect. 5.

## 4 Study of nuclei close to the proton drip line

Recently, our interest was focused on the study of nuclei close to the proton drip line in the $A \sim 130$ mass region, with the aim to determine their lowest-lying configurations. The study was motivated by the need to have experimental data in nuclei as close as possible to the unknown Pr and Pm proton emitters in this mass region, in order to make realistic predictions for the lifetimes of the emitting states. An experiment was performed using a self-supporting 0.5 mg/cm$^2$ thick $^{92}$Mo target with a 190 MeV $^{40}$Ca beam of 5 pnA intensity. The beam was provided by the XTU Tandem accelerator of the Laboratori Nazionali di Legnaro and the experimental setup consisted of the GASP array for $\gamma$-ray detection and the ISIS ball for charged-particle detection. New results were obtained on many nuclei close to the proton drip line, in which we were able to identify excited states up to unexpected high spins. We observed, for the first time, excited states in $^{126}$Pr [22], constructed a detailed level scheme and identify a pair of bands with nearly degenerate levels in $^{128}$Pr [17], constructed a detailed level scheme of $^{122}$Ba [23], identify several rotational bands in $^{128}$Nd [24], constructed detailed level schemes for $^{125}$Ce [25] and $^{126}$Ce [26]. The band structures observed in $^{126}$Pr, $^{125}$Ce and $^{126}$Ce were interpreted with the Interacting Boson Model + Broken Pairs model, which resulted to be successful in describing the high-spin states the light $A \sim 130$ deformed nuclei (see fig. 6 taken from ref. [25]).

## 5 The origin of doublet bands in odd-odd Pr nuclei

The possibility of chirality in triaxial rotating nuclei predicted theoretically by Frauendorf [27,28], results from a combination of geometry (triaxial nucleus) and dynamics (total angular momentum). The angular momentum vector introduces chirality by selecting one of the octants of the space, giving rise to two degenerate rotational bands. This nice model brought the neutron-deficient odd-odd Pr nuclei and their neighbors into the focus of experimental studies, since one of the best examples of broken chiral symmetry up to date is $^{134}$Pr. Extensive studies were performed in several laboratories around the world, and other candidates for chiral doublet bands were proposed [29]. However, the $^{134}$Pr nucleus remained the only case where

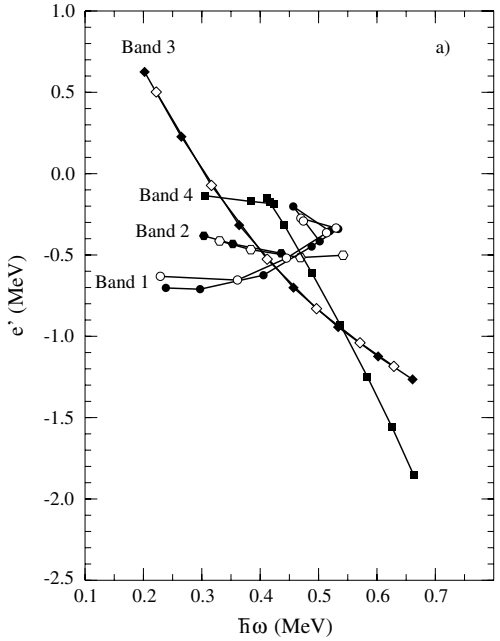


**Fig. 7.** Experimental Routhians for the observed bands in $^{134}$Pr. The bands with signature $\alpha = 0$ ($\alpha = 1$) are drawn with filled (open) symbols.

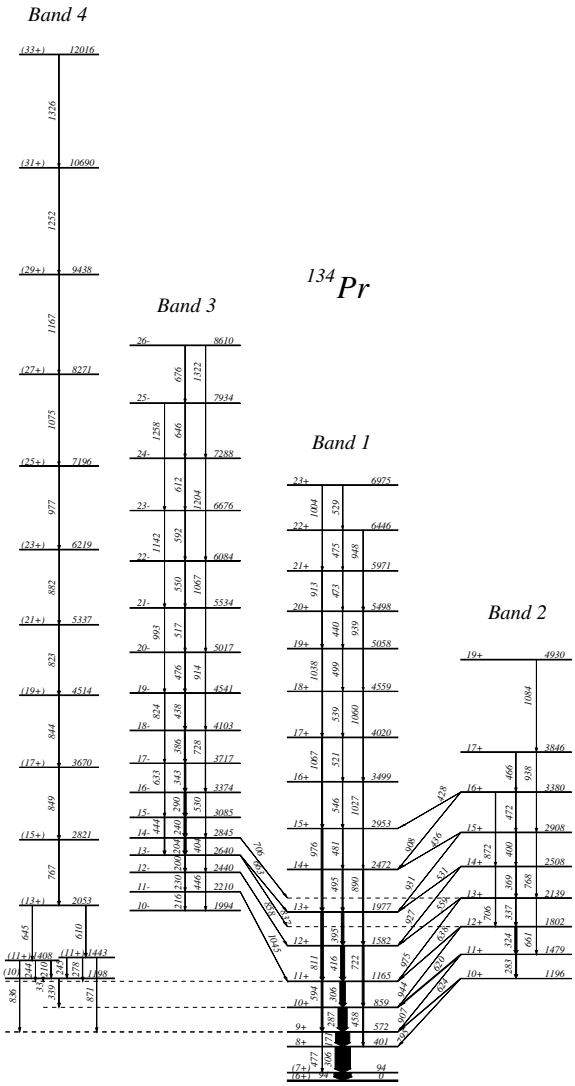


**Fig. 8.** Decay scheme of $^{134}$Pr.

the behaviour of the doublet bands was considered to approach the model predictions.

In the present discussion I would like to remind the main features of the observed doublet bands in $^{134}$Pr and stress that we have not yet a good example of broken chiral symmetry in nuclei. In the following we will call band 1 and band 2 the lowest observed bands in $^{134}$Pr [14]. The lowest observed state of band 2 ($10^+$) lies 337 keV above the $10^+$ state of band 1. Band 2 crosses band 1 at spin $14^+$, which corresponds to a rotational frequency of around 0.45 MeV (see fig. 7). As one can see in fig. 8, the two bands are nearly degenerate only on a very limited spin range, as is the case of many rotational bands built on different shapes or configurations. The single-particle alignment of band 2 is larger by $2\hbar$ units than that of band 1 (see fig. 9), as one would expect, for example, for a $\gamma$-vibration built on the configuration of band 1. Band 1 exhibits a backbending at a rotational frequency of about 0.5 MeV, which strongly disturbs the regularity of the band at high spins. This also contributes to the very limited spin range in which the properties of the possible chiral candidates remain undisturbed. In particular, this is the reason for which the $B(M1)/B(E2)$ predictions of the 3D TAC model cannot be compared in a straightforward manner to the experimental values in $^{134}$Pr. In order to understand the structure of the two bands, we performed Total Routhian Surface calculations based on the Cranked Shell Model with a Woods-Saxon potential and two-particle plus triaxial rotor calculations [14]. As can be seen in fig. 10, the minima are very flat in the $\gamma$ degree of freedom, the barrier between the minima with positive and negative $\gamma$ being of the order of 200 keV. Possible descriptions of the two bands involve either shape coexistence in terms of different $\gamma$-deformation of the two structures or the coupling to the $\gamma$-phonon. Within the mentioned calculations we were not able to find a consistent interpretation of bands 1 and 2 of $^{134}$Pr. However, one cannot be satisfied with the description in terms of chiral doublet bands, because the experimental features of the bands can be due to a subtle superposition of various effects, leading to a simple near degeneracy of a few levels in the region of band crossing. It is therefore necessary to continue the search for doublet bands in odd-odd nuclei, to find a good example of broken chiral symmetry in nuclei.

Another origin of doublet bands in odd-odd nuclei, with characteristics slightly different than the claimed chiral doublets, is the pseudospin symmetry [30]. In the pseudospin formalism one assigns new spin and orbital momentum labels to the single-particle levels in accordance with an observed near degeneracy of certain normal-parity eigenstates (pseudospin doublets) of the spherical nuclear mean field. It could be that for particular nucleon numbers the Fermi level lies just between the two members

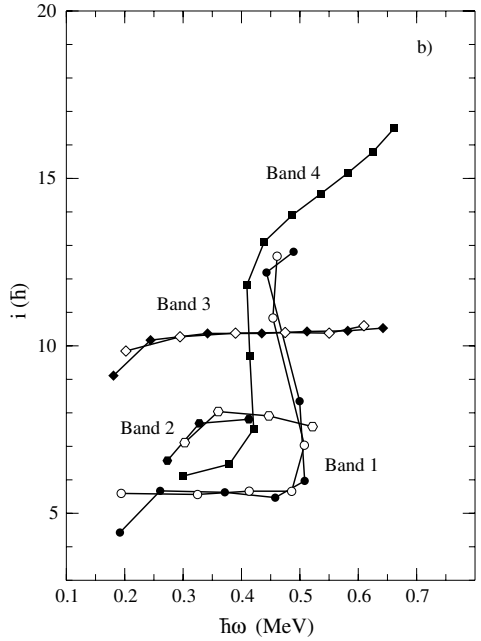


**Fig. 9.** Experimental alignments for the observed bands in $^{134}$Pr. The bands with signature $\alpha = 0$ ($\alpha = 1$) are drawn with filled (open) symbols.

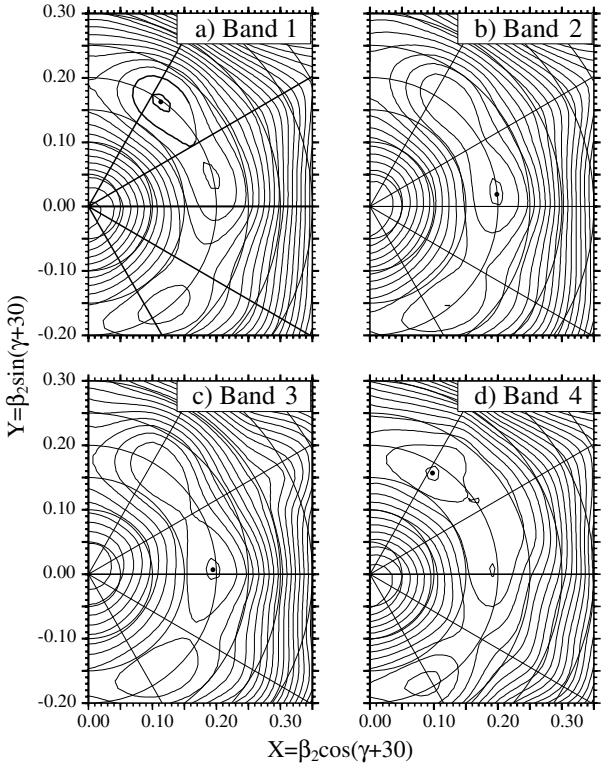


**Fig. 10.** Total Routhian Surface (TRS) calculations for the different configurations assigned to the observed bands in $^{134}$Pr for $\omega = 0.112$ MeV/$\hbar$.

of the pseudospin members, giving rise to bands with levels which are nearly degenerate. One such case is suggested to occur in the odd-odd $^{128}$Pr nucleus [17], in which the proton Fermi level is expected to lie close to the [420]1/2$^+$-[422]3/2$^+$ doublet of mixed $d_{5/2}/g_{7/2}$ composition, leading to the [3$\tilde{2}$1] pseudospin doublet. However, both in a Tilted Axis Cranking and a Two-quasiparticle Rotor calculations including the residual n-p interaction, it turned out to be impossible to achieve the observed small level spacing and the staggering (see fig. 11). If the observed close spacing is not restricted to $^{128}$Pr, but appears in a systematic way, it could be due to some accidental combination of effects not taken into account in the standard models and may be a hint of a hidden symmetry to be revealed.

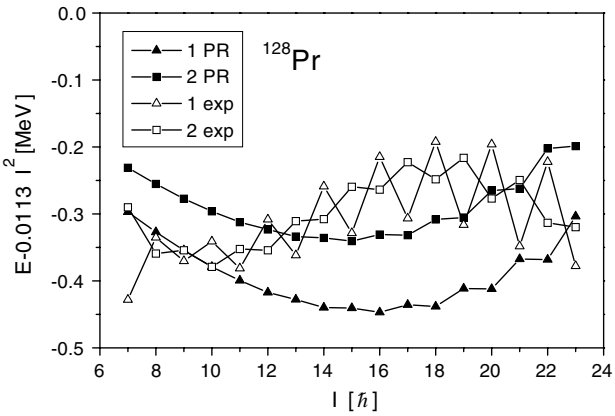


**Fig. 11.** Comparison of two-quasiparticle+rotor calculation with the experimental energies of the band 1 and 2. The parameters are $\varepsilon = 0.265$, $\gamma = 0°$, and $\varepsilon_4 = 0.02$, $\Delta_p = 1.04$ MeV and $\Delta_n = 1.06$ MeV. A Coriolis attenuation factor of 0.7 is used and the moment of inertia of the rotor is adjusted to the experiment.

## 6 Conclusions

In our recent studies with GASP we have shown that very high spins can be populated in nuclei close to the proton drip line, allowing a detailed spectroscopy much farther away from the stability line than previously thought. The study of the doublet bands in the odd-odd nuclei showed that their origin can be traced back to either chiral or pseudospin symmetry. The need to search for good examples of chiral doublet bands in odd-odd nuclei remains an imperative for future studies. However, one should not limit our interest only to odd-odd nuclei, because, in principle, the chiral regime can be achieved also in even-even or odd-even nuclei.

I am highly indebted to the GASP group, and in particular to Dino Bazzacco, Santo Lunardi and Carlos Rossi Alvarez, which assured the smooth operation of the setup during the experiments we performed in the last decade, and to the accelerator group of LNL for delivering high-quality beams. I would like to mention the essential contribution to the understanding of the obtained results of Ramon Wyss and Ingemar Ragnarsson, as well as Slobodan Brant and Dario Vretenar.

## References


1. D. Bazzacco *et al.*, Phys. Lett. B **309**, 235 (1993).
2. C.M. Petrache *et al.*, Phys. Lett. B **335**, 307 (1994).
3. S. Lunardi *et al.*, Phys. Rev. C **52**, R6 (1995).
4. C.M. Petrache *et al.*, Phys. Rev. Lett. **77**, 239 (1996).
5. C.M. Petrache *et al.*, Phys. Lett. B **383**, 145 (1996).
6. C.M. Petrache *et al.*, Phys. Lett. B **387**, 31 (1996).
7. C.M. Petrache *et al.*, Phys. Lett. B **415**, 223 (1997).
8. C.M. Petrache, Zeit. Phys. A **358**, 225 (1997).
9. C.M. Petrache *et al.*, Phys. Rev. C **57**, R10 (1998).
10. M.N. Rao *et al.*, Phys. Rev. C **58**, R1367 (1998).
11. C.M. Petrache *et al.*, Phys. Rev. C **58**, R611 (1998).
12. S. Perriés *et al.*, Phys. Rev. C **60**, 064313 (1999).
13. C.M. Petrache *et al.*, *Nuclear Structure 98*, edited by C. Baktash (AIP, Woodbury, New York, 1999), AIP Conf. Proc. **481**, 31 (1999).
14. C.M. Petrache *et al.*, Nucl. Phys. A **597**, 106 (1996).
15. C.M. Petrache *et al.*, Nucl. Phys. A **603**, 50 (1996).
16. C.M. Petrache *et al.*, Nucl. Phys. A **635**, 361 (1998).
17. C.M. Petrache *et al.*, Phys. Rev. C **65**, 054324 (2002).
18. C.M. Petrache *et al.*, Phys. Lett. B **373**, 275 (1996).
19. C.M. Petrache *et al.*, Nucl. Phys. A **617**, 228 (1997).
20. C.M. Petrache *et al.*, Phys. Rev. C **61**, 011305 (2000).
21. D. Madland, J. Nix, Nucl. Phys.A **476**, 1 (1988).
22. C.M. Petrache *et al.*, Phys. Rev. C **64**, 044303 (2001).
23. C.M. Petrache *et al.*, Eur. Phys. J. A **12**, 135 (2001).
24. C.M. Petrache *et al.*, Eur. Phys. J. A **12**, 139 (2001).
25. C.M. Petrache *et al.*, Eur. Phys. J. A **14**, 439 (2002).
26. C.M. Petrache *et al.*, Eur. Phys. J. A **16**, 337 (2003).
27. S. Frauendorf, J. Meng, Nucl. Phys. A **617**, 131 (1997).
28. V.I. Dimitrov, S. Frauendorf, F. Dönau, Phys. Rev. Lett. **84**, 5732 (2000).
29. K. Starosta *et al.*, Nucl. Phys. A **682**, 375c (2001).
30. A. Bohr, I. Hamamoto, B. Mottelson, Phys. Scr. **26**, 267 (1982).